

## Role of Electric Field in the Formation of Detached Regime

I.Senichenkov<sup>1</sup>, E. Kaveeva<sup>1</sup>, V. Rozhansky<sup>1</sup>, E. Sytova<sup>1</sup>, I. Veselova<sup>1</sup>,  
S. Voskoboynikov<sup>1</sup>, D. Coster<sup>2</sup>

<sup>1</sup>Peter the Great St.Petersburg Polytechnic University, Saint Petersburg, Russia

<sup>2</sup>Max-Planck Institut für Plasmaphysik, EURATOM Association, Garching, Germany

The detached regime of divertors is considered now as the main working regime of ITER, and the physics of its formation is actively studied experimentally [1-3] and theoretically [4].

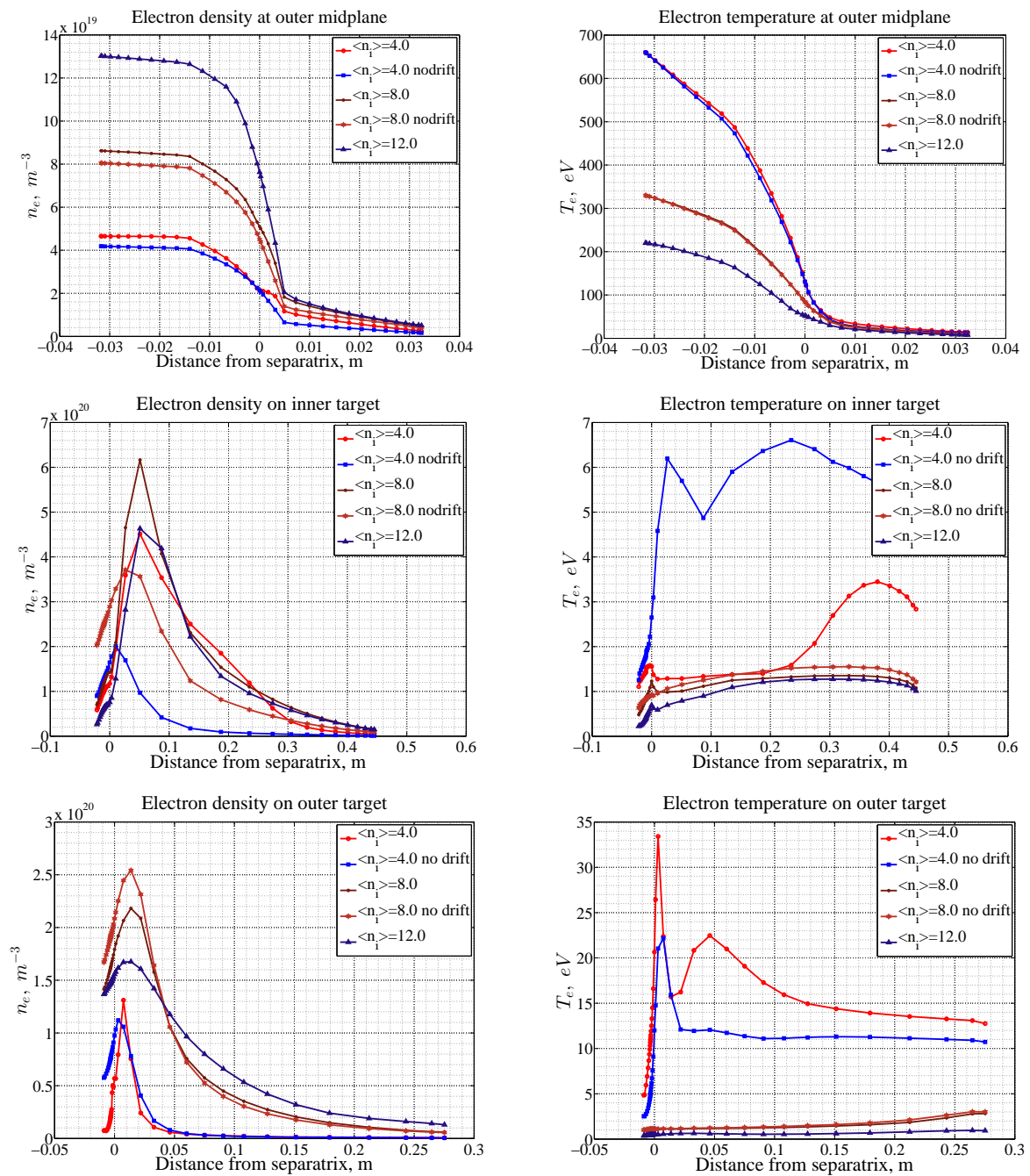


Figure 1: Outer midplane and divertor profiles of electron density and temperature for all the runs considered. Here and later on runs are labeled by core boundary density of deuterium.

In the present report the role of electric field and corresponding  $\vec{E} \times \vec{B}$  drift and currents in the detached regime formation is studied using modeling with the SOLPS-ITER code [5]. As a base modeling scenario the ASDEX Upgrade shot #17151 (with carbon impurity) was chosen, then the transition to detachment was modelled by increasing the density at the core boundary of computational domain and a corresponding decreasing of temperatures keeping the product  $n_e(T_e + T_i)$  constant. Total power through separatrix  $P \approx 3$  MW (without radiation) was the same for all variants. Additionally runs were made with drifts turned off as reference cases, see Figs 1 and 2. For  $\langle n_i \rangle = 4.0 \cdot 10^{19} \text{ m}^{-3}$  the inner divertor is detached and outer is in high recycling regime. For  $\langle n_i \rangle = 8.0 \cdot 10^{19} \text{ m}^{-3}$  and  $\langle n_i \rangle = 12.0 \cdot 10^{19} \text{ m}^{-3}$  the outer divertor also becomes detached. As the core density increases, the particle flux first increases too (being proportional to saturation current), and then falls down, i.e. the rollover occurs.

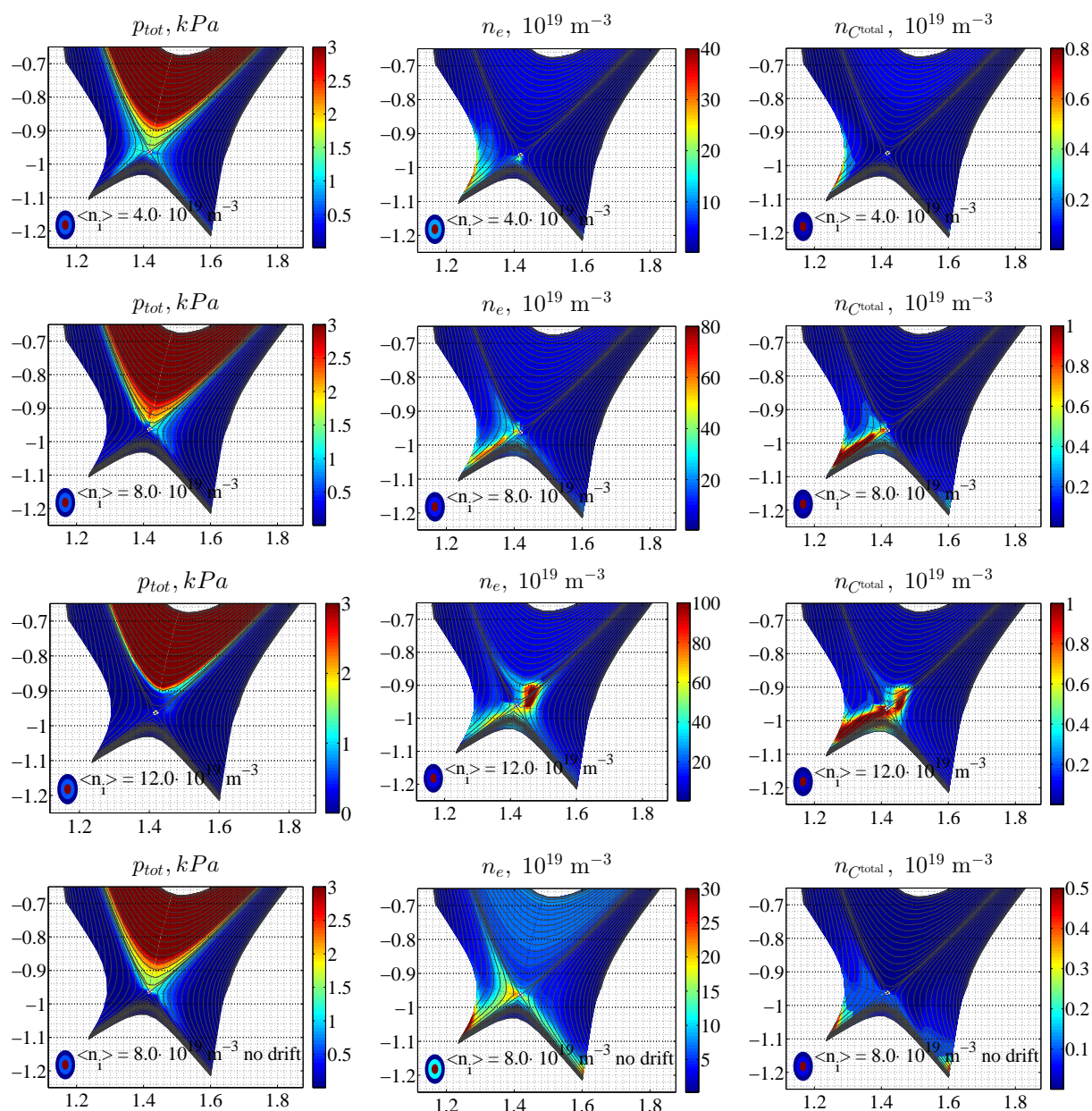


Figure 2. Total pressure, electron and carbon density in several runs

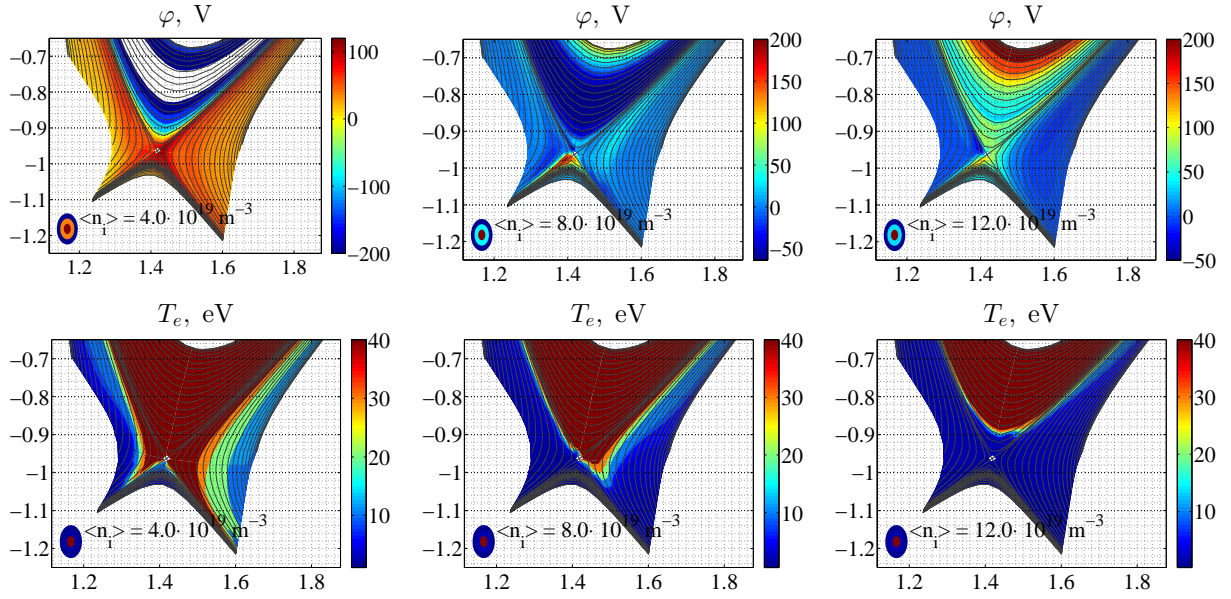


Figure 3. Electrostatic potential and electron temperature for runs with  $\langle n_1 \rangle = 4.0, 8.0, 12.0 \times 10^{19} \text{ m}^{-3}$

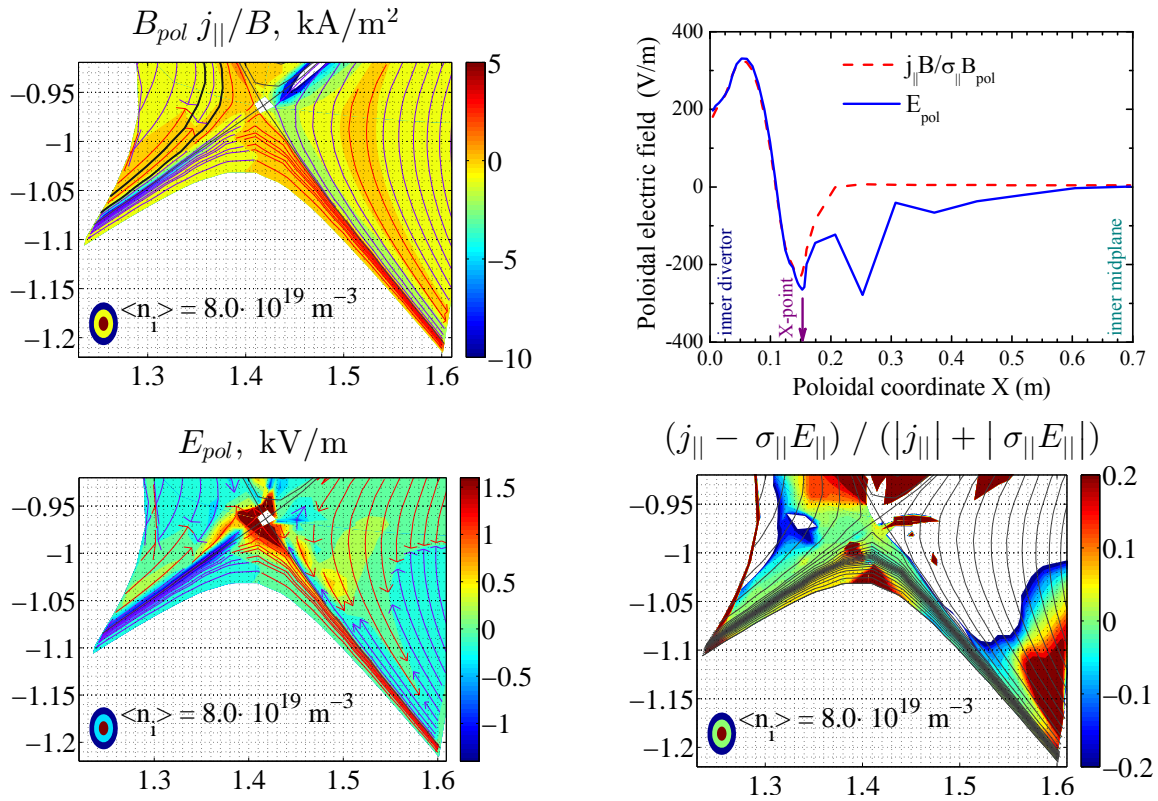


Figure 4. Left top: Poloidal projection of parallel current density, colour arrows represent the direction. Left bottom: Poloidal electric field. Right top: Poloidal electric field along flux surface lying between two bold curves on left top graph. Right bottom: Zones where the relation  $j_{||} \approx \sigma_{||} E_{||}$  is satisfied.

It is demonstrated that the typical feature of a detached regime of a divertor is the formation of rather strong potential in the divertor region, up to 100 V, which can be order of magnitude larger than  $T_e/e$ , see Figure 3. Strong poloidal electric fields in the cold regions of low Spitzer conductivity are required to provide parallel current  $j_{||} = \sigma_{||} (E_{||} + \nabla_{||} (n_e T_e) / n_e + 0.71 \nabla_{||} T_e / e)$ . Thus, in contrast to attached divertor, where electric field balances electron pressure gradient

and thermal force, so that  $E_{\parallel} + \nabla_{\parallel}(n_e T_e)/en_e + 0.71\nabla_{\parallel}T_e/e \approx 0$  and  $E_{\parallel}$  is of the order of  $\nabla_{\parallel}T_e/e$ , in the detached regime the relation  $j_{\parallel} \approx \sigma_{\parallel}E_{\parallel}$  is satisfied in the cold region, and  $|E_{\parallel}|$  becomes much larger than  $|\nabla_{\parallel}T_e|/e$ , see Fig. 4. The parallel current is the sum of parallel Pfirsch-Schlüter current which closes vertical  $\nabla B$  driven current and thermal current flowing from the hotter to the colder divertor. Note that when both inner and outer divertors fall into detached regime, the thermal current is reduced significantly compared with the case when at least one divertor is attached. This results in the significant reduction of the net current on divertor plates down to values comparable with total radial currents through the outer SOL and PFR boundaries of computational domain, see Figure 5. Strong radial electric field also

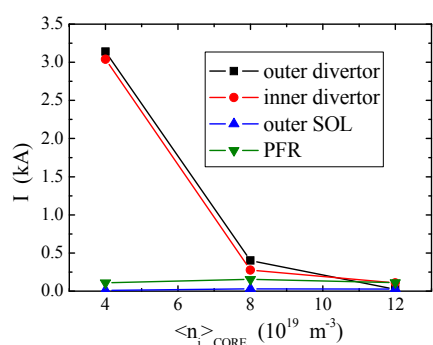


Figure 5. Net current through boundaries of computational domain.

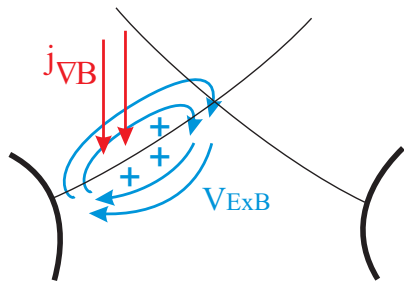


Figure 6. Scheme of  $\vec{E} \times \vec{B}$  vortex flow. (Fig. 4), since it is determined by the parallel current, required to compensate PS and thermal currents, and therefore E-field could change sign.

## Conclusions

It is demonstrated that in the detached regimes strong electric field and  $\vec{E} \times \vec{B}$  drift arise, which are completely different from those in high recycling regimes. The radial  $\vec{E} \times \vec{B}$  drifts are comparable with the diffusive fluxes and responsible for density redistribution along the plates and near the X-point.

## References

- [1] S. Potzel et al., Nucl. Fusion **54** (2014) 013001
- [2] F. Reimold et al., Nucl. Fusion **55** (2015) 033004
- [3] A. Kallenbach et al, Nucl. Fusion **55** (2015) 053026
- [4] F. Reimold et al., Journal of Nuclear Materials 463 (2015) 128–134
- [5] S. Wiesen et al., Journal of Nuclear Materials 463 (2015) 480–484